PCCP

Direct studies on the decomposition of the *tert*-butoxy radical and its reaction with NO

M. Blitz,[a] M. J. Pilling,[a] S. H. Robertson[b] and P. W. Seakins*[a]

[a] *School of Chemistry, University of Leeds, Leeds, UK LS2 9JT*
[b] *Molecular Simulations Inc, The Quorum, Barnwell Road, Cambridge, UK*

Received 18th August 1998, Accepted 12th October 1998

The first laser induced fluorescence (LIF) spectrum for the *tert*-butoxy radical is reported following radical generation by excimer laser photolysis of *tert*-butyl nitrite. The laser flash photolysis-LIF technique is used to measure the temperature dependence of the rate coefficient for the reaction with NO (T = 200–390 K):

$$(CH_3)_3CO + NO \rightarrow (CH_3)_3CONO \quad (3)$$

which can be represented in either Arrhenius or AT^{-n} format:

$$k_3 = (7.8 \pm 1.8) \times 10^{-12} \exp(2850 \pm 290 \text{ J mol}^{-1}/RT) \text{ cm}^3 \text{ molecule}^{-1} \text{ s}^{-1}$$

$$k_3 = (4.17 \pm 0.12) \times 10^{-11}(T/200)^{-1.27 \pm 0.07} \text{ cm}^3 \text{ molecule}^{-1} \text{ s}^{-1}$$

and the *tert*-butoxy decomposition.

$$(CH_3)_3CO \rightarrow CH_3COCH_3 + CH_3 \quad (2)$$

Whilst the former reaction shows no pressure dependence (p = 70–500 Torr of helium), the latter reaction is in the fall-off regime over the entire range of experimental conditions (T = 303–393 K, p = 13–600 Torr helium). The fall-off data were fitted using an inverse Laplace transformation/master equation model to give the following Arrhenius parameters:

$$k_2^{\infty}(T) = (1.4 \pm 0.6) \times 10^{13} \exp[-(57 \pm 2) \text{ kJ mol}^{-1}/RT]$$

These Arrhenius parameters are significantly lower than previous indirect measurements or calculations and the atmospheric and mechanistic implications are discussed.

Finally, reaction (3) was also studied by monitoring the temporal dependence of the NO LIF signal following the photolysis of *tert*-butylnitrite with no additional NO. The results are in good agreement with the *tert*-butoxy monitoring and allow for an estimation of the rate parameters for the *tert*-butoxy self reaction.

I Introduction

Alkoxy radicals are mechanistically important in the low temperature oxidation of hydrocarbons.[1,2] In general three reactions are possible: decomposition (1a), isomerization (1b) and reaction with oxygen (1c)

$$RO \rightarrow \text{carbonyl} + \text{alkyl radical} \quad (1a)$$

$$RO \rightarrow {}^{\cdot}R'OH \quad (1b)$$

$$RO + O_2 \rightarrow HO_2 + \text{carbonyl} \quad (1c)$$

These different reaction pathways can have significant effects determining, for example, the number of NO to NO_2 conversions that can take place during the oxidation of the parent hydrocarbon in the atmosphere and hence affecting tropospheric ozone production. Despite the importance of alkoxy reactions, only reactions of the methoxy radical have been reasonably well characterised; there have been very few direct studies of larger alkoxy radicals. This dearth of information stems both from difficulties in cleanly generating, and sensitively monitoring, alkoxy radicals.

As part of a larger consortium[3] investigating the reactions of biogenic hydrocarbons, we have started a systematic study of the reactions of C_4 alkoxy radicals using laser flash photolysis for alkoxy generation coupled with laser induced fluorescence (LIF) detection, primarily of the reaction products. The *tert*-butoxy radical is an obvious starting point as the lack of α-hydrogens and the geometry of the radical means that reactions with O_2 and internal abstraction (isomerization) are extremely unlikely, and hence the only reaction of atmospheric significance is the decomposition to acetone and methyl radical [reaction (2)].

$$(CH_3)CO \rightarrow CH_3COCH_3 + CH_3 \quad (2)$$

The study of *tert*-butoxy reactions is further simplified as it was possible to obtain a LIF spectrum of C_4H_9O allowing direct detection of the radical reagent.

The majority of the previous work on *tert*-butoxy decomposition has been performed by Batt and co-workers.[4–8] Either thermal decomposition or photolysis was used to generate alkoxy radicals and rate coefficients were extracted following end product analysis by gas chromatography. The Arrhenius parameters generated in this current work are different from Batt's earlier work. The mechanistic implications of the low A factors and activation energies are discussed in Section V, along with a consideration of the atmospheric implications.

In the atmosphere, reactions (1a–c) dominate the kinetics of alkoxy removal. However, in the laboratory, alkoxy reactions

often occur in the presence of NO, either from the photolysis or decomposition of a nitrite alkoxy precursor or as an added reagent, and hence reactions of alkoxy radicals with NO are of interest. Although there are no direct studies of the NO reaction with *tert*-butoxy, the reactions with methoxy, ethoxy and isopropoxy radicals have been studied and hence provide a bench mark against which we can judge the validity of our technique. The rate coefficients are relatively invariant with the size of the alkoxy species and Atkinson[1] has suggested a common Arrhenius expression for the reaction of all alkoxy radicals with NO. The reaction was studied in two ways, firstly by direct observation of the reaction of *tert*-butoxy with an excess of NO; and secondly by monitoring the concentration of NO following the photolysis of the *tert*-butoxy nitrite precursor. In conjunction with the decomposition measurements this second method allows for the simultaneous estimation of the *tert*-butoxy self reaction.

The paper is structured as follows. In Section II we describe the experimental apparatus and techniques used to monitor the decomposition and reaction of *tert*-butoxy with NO. Section III describes the observed laser-induced fluorescence spectrum and Section IV details the results of the studies of the reaction of *tert*-butoxy with excess NO. In Section V the results of the study of the *tert*-butoxy decomposition reaction between 303 and 393 K are presented and the implications of the resulting Arrhenius parameters are discussed. The results of NO monitoring experiments are presented in Section VI and finally the work is summarised in Section VII.

II Experimental

All experiments were undertaken in a conventional slow flow, laser flash photolysis-laser induced fluorescence apparatus, similar to that used in previous experiments.[9] *tert*-Butoxy and NO were generated *via* the pulsed excimer laser (Lambda Physik LPX 100) photolysis of *tert*-butyl nitrite at 351 nm (XeF). In experiments where *tert*-butoxy was monitored the laser repetition rate was 3 Hz, but in experiments monitoring the time dependence of the NO concentration a slower repetition rate of 0.3 Hz was used to ensure that the complete contents of the cell were flushed between laser shots. The photolysis energy was approximately 100 mJ pulse^{-1} contained within a beam *ca.* 2 × 1 cm in size.

The probe light was generated from a Nd:YAG (Spectron SL803, doubled output at 532 nm) pumped dye laser, using appropriate doubling/mixing (KDP) crystals. For *tert*-butoxy observation, the light output from a Pyridine 1 dye (670–720 nm) was doubled to probe a range of *tert*-butoxy features (See below). For NO observation, the output from the dye laser (Rhodamine 6G) was doubled and then mixed with the fundamental (1064 nm) from the Nd:YAG laser to generate light *ca.* 226 nm. NO was probed in the P2 branch head of the $A\,^2\Sigma \leftarrow X\,^2\Pi$ band system near 226.87 nm. The probe light was $\leqslant$1 mJ pulse^{-1} and intersected the photolysis laser beam at right angles.

Laser induced fluorescence was collected by a photomultiplier (EMI 9813 QKB) perpendicular to both the photolysis and probe beams and the resulting signal was integrated using a boxcar averager (SRS SR250) minimising scattered light. For NO monitoring the fluorescence was filtered by a monochromator centred on the probe beam wavelength and for the *tert*-butoxy experiments, a Perspex filter collected light at wavelengths greater than 390 nm. The integrated signal was subsequently digitised and stored on a PC. The radical time-profiles were accumulated by scanning the delay between the photolysis and probe lasers with each kinetic trace containing 100 time points, and each point being the average of 4–10 laser samples.

Gas flows were measured using calibrated flow controllers and mixed in a manifold prior to entering the reaction cell. The pressures in the cell were monitored using capacitance manometers, and varied by throttling the exit valve on the cell. High total flow rates ($\sim$750 sccm) were used in the NO experiments, the buffer gases for the experiments being either helium or helium–methane mixtures. For the *tert*-butoxy experiments lower flow rates could be used and pressures were varied between 15–600 Torr using helium as the buffer gas. Sub ambient temperatures were obtained by flowing suitable coolants around the outside of the reactor, high temperatures were obtained using cartridge heaters located in the metal block situated around the centre of the reaction cell. Temperatures were measured using two thermocouples (type K) located just above and below the reaction zone. Temperatures could be controlled to better than $\pm$1 K.

tert-Butylnitrite (Aldrich, 98%) was thoroughly degassed, diluted in helium and stored in blackened 5 l glass bulbs. NO (Linde, 99%) was distilled at 196 K to remove NO_2 and then diluted in helium before storage in darkened bulbs. Helium (CP grade, 99.999%, BOC) and methane (UHP, 99.995% Linde) were used directly from the cylinders.

III *tert*-Butoxy spectrum

Photolysis of *tert*-butylnitrite, (60 mTorr in 70 Torr of helium) produced a species that fluoresces with considerable red shift when probed between *ca.* 330–360 nm. The lifetime of the observed signal was *ca.* 500 ns. The use of a Perspex filter which transmits light at wavelengths greater than 390 nm removes any scattered light. Significantly red shifted fluorescence is characteristic of lower alkoxy radicals.[10–12] A spectrum of the observed species was recorded: the signal was obtained with a 50 μs delay between the photolysis and probe lasers and the cell was cooled to 203 K in order to sharpen the spectrum which is displayed in Fig. 1. This spectrum is broadly similar to other alkoxy spectra but quantitatively different, *i.e.* it does not arise from lower alkoxy radicals formed in alternative photochemical reactions. Whilst the spectrum is broad, it does appear to have vibrational structure, with two progressions, and a separation within each progression of approximately (500 $\pm$ 20) cm^{-1}. This type of vibrational progression is observed in other alkoxy radicals and has been assigned to the C–O stretch in the excited state. There appears to be a gradual decrease in the frequency of stretch with the size of the alkoxy radical (ethoxy 590 cm^{-1},[11] isopropoxy 560 $\pm$ 10 cm^{-1} [10]) which may be due to a combination of weakening bond strength and change in mass of the alkyl fragment. The apparent fine structure is an artefact of the doubling crystal autotracker.

The time dependence of the intensities of the 5 strongest peaks of the spectrum in the presence of added NO all gave decay constants that were the same within experimental error

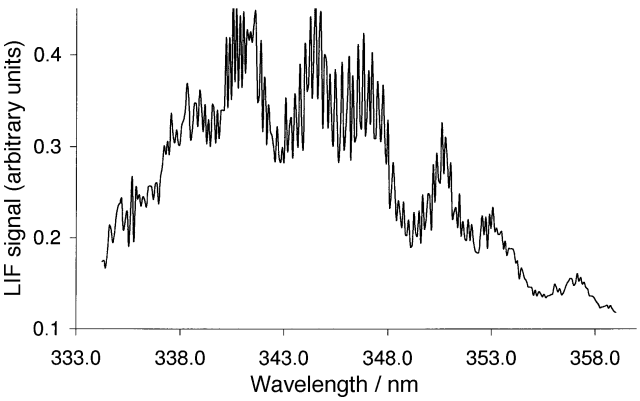

Fig. 1 *tert*-Butoxy excitation spectrum monitored by recording the total fluorescence passing through a Perspex filter. Conditions: 203 K, $\sim$100 mTorr of *tert*-butoxynitrite, 70 Torr total pressure of helium.

indicating that all of the spectrum shown in Fig. 1 arises from a single species.

Photolysis of the C_1–C_3 alkyl nitrites is an established method of generating the corresponding alkoxy radical and there is no reason to expect that *tert*-butylnitrite should be any different. This is supported by earlier end product analysis studies following the photolysis of *tert*-butylnitrite[8] where the results are entirely consistent with reactions of the *tert*-butoxy radical.

In the absence of a complete spectral assignment it is impossible to positively identify the observed spectrum with the *tert*-butoxy radical, however, spectroscopic and chemical evidence indicate that this is a reasonable assumption and it is difficult to postulate any other species which could give the observed fluorescence spectrum with the time dependence presented in subsequent sections.

IV Results for the reaction of *tert*-butoxy + NO

Initial experiments on reaction (3) were performed in a conventional manner, with the

$$(CH_3)_3CO + NO \rightarrow (CH_3)_3CONO \qquad (3)$$

decay of the *tert*-butoxy LIF signal being monitored in the prescence of a large excess of NO. Further information on the reaction obtained by monitoring the time dependence of NO produced in the photolysis pulse is given in Section VI. A typical decay trace and a range of bimolecular plots are shown in Fig. 2. In all cases the decays were exponential and Fig. 2b shows that the bimolecular plots are linear as [NO] is varied, typically by a factor of 10. No pressure dependence was observed [p(He) = 70–600 Torr].

Experiments were repeated over the temperature range 200–390 K and the temperature dependence of the reaction is depicted in Fig. 3. The data can conveniently be represented in either Arrhenius or AT^{-n} format:

$$k_3 = (7.8 \pm 1.8) \times 10^{-12} \times \exp(2850 \pm 290 \text{ J mol}^{-1}/RT) \text{ cm}^3 \text{ molecule}^{-1} \text{ s}^{-1}$$

$$k_3 = (4.17 \pm 0.12) \times 10^{-11}(T/200)^{-1.27} \pm 0.07 \text{ cm}^3 \text{ molecule}^{-1} \text{ s}^{-1}$$

Unlike primary and secondary alkoxy radicals, abstraction of an α hydrogen by NO is impossible in the *tert*-butoxy system (and β abstraction will probably be extremely slow), however, instead of recombination to reform the nitrite, it could be possible to form *tert*-$C_4H_9NO_2$ but this is considered to be unlikely. Zellner[14] has studied the recovery of CH_3ONO and saw no evidence for the formation of CH_3NO_2, which would be expected to require a significant energy barrier for formation.

Table 1 shows that the room temperature value determined in this study is consistent with other alkoxy reactions. The temperature dependence of the reaction is slightly greater than that predicted by Atkinson's universal parameters[1] and the results from Table 1 do seem to suggest a very slight increase in the temperature dependence of the reactions with increasing size of the alkoxy radical, a trend which would be predicted from current theories of recombination reactions.[15] The earlier work on the smaller alkoxy reactions showed that the reaction with NO was at the high pressure limit at 15 Torr,[11] and the lack of any pressure dependence in this study is consistent with these observations.

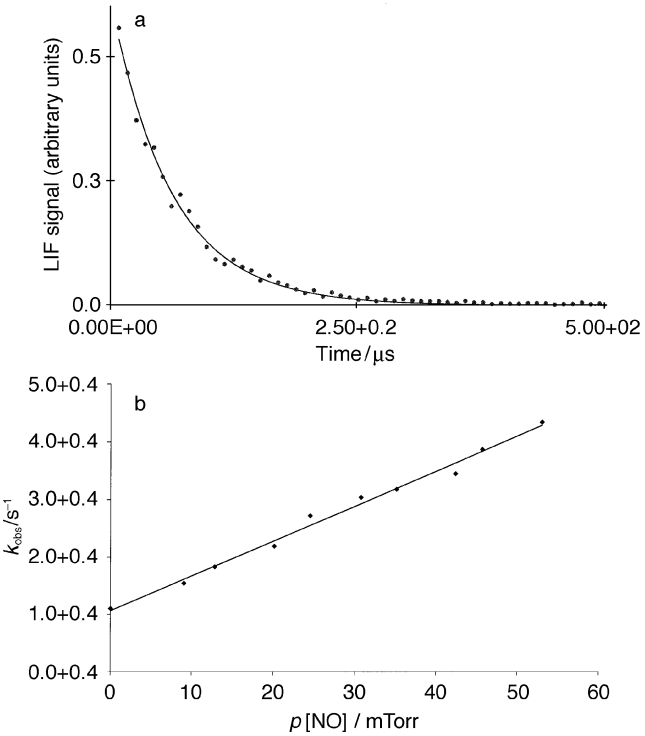

Fig. 2 a, Typical *tert*-butoxy decay trace following the photolysis of 60 mTorr of *tert*-butyl nitrite in the presence of 9.1 mTorr of NO at a total pressure of 71 Torr of helium at 333 K; b, typical bimolecular plot showing the variation of pseudo-first-order rate coefficient with [NO] at 333 K.

Given that recombination is the only possible outcome of the *tert*-butoxy + NO reaction, the measured activation energy could, in theory, be used in conjunction with the reverse decomposition data to estimate the overall reaction enthalpy and hence the heat of formation of the *tert*-butoxy radical. However, in practice there are difficulties with this ap-

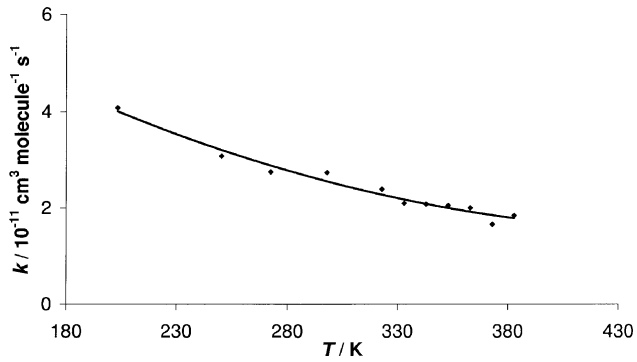

Fig. 3 Temperature dependence of the reaction of *tert*-butoxy with NO.

Table 1 Arrhenius parameters and k_{298} values from direct studies of the reaction of alkoxy radicals with NO

Radical	10^{11} A/cm^3 molecule^{-1} s^{-1}	E/kJ mol^{-1}	10^{11} k_{298}/cm^3 molecule^{-1} s^{-1}	Reference
C_2H_5O			4.4 ± 0.4	11
C_2H_5O	1.9	−1.7	3.8	13
iso-C_3H_7O	1.22	−2.6	3.5	10
tert-C_4H_9O	0.8	−2.85	2.5	This work
All	2.3	−1.25	3.8	1

proach. Firstly, there is considerable variation (± 5 kJ mol^{-1}) in the activation energy for the decomposition reaction of the nitrite[16–18] and secondly, the enthalpy of formation of the *tert*-butylnitrite molecule has not been measured. A value for the enthalpy of formation of the nitrite could be estimated from group additivity,[19] however, a comparison of the measured and estimated values for the heat of formation of methyl and ethyl nitrite indicates an approximate uncertainty of ± 3 kJ mol^{-1} in the value of the O–NO/C group. The precision of any resulting calculation will therefore not be an improvement on the current recommended heat of formation for the *tert*-butoxy (-90.7 kJ mol^{-1}) proposed by McMillan and Golden.[20]

V *tert*-Butoxy decomposition

The decomposition reaction has been studied from 303–393 K. Within this range the reaction

$$(CH_3)_3CO \rightarrow CH_3COCH_3 + CH_3 \qquad (2)$$

was found to be pressure dependent and for each temperature the reaction was studied between pressures of 13 and 600 Torr of helium. For a given pressure and temperature the decays were always exponential in nature. At low temperatures a slight correction had to be introduced due to the reaction of the alkoxy radical with residual NO, however, this correction was always small. The highest temperature was limited by the speed of the reaction and the need to ensure that vibrational relaxation of the *tert*-butoxy radical was complete before decomposition occurred. Examples of the pressure dependence are shown as the solid points in Fig. 4.

From our study it is not possible to unequivocally state that we are observing the decomposition reaction, there is a small possibility that some reagent is being removed by an alternative first order process such as a 1,4 isomerization. However decomposition is by far the most likely route as it will have a significantly lower activation energy. Previous end product analyses of the decomposition reaction[8] have shown no evidence of an alternative first order removal process.

In order to investigate the pressure dependence of this reaction and to extract Arrhenius parameters for the limiting high pressure rate coefficient, k_2^{∞}, we have modelled the experimental data using two methods: the inverse Laplace transform-master equation technique (ILT-ME)[15] and the Troe factorisation formulation.[21–23]

For the ILT-ME method the geometry, frequencies and rotational barriers were calculated using the Cerius2 program.[24] The universal force-field was used together with the charge equilibrium[25] module to construct a potential energy surface. The molecular geometry was obtained by minimising the potential energy (charges were recalculated periodically). Once the minimum structure was obtained, the frequencies were obtained in the usual way.[26] The lower three frequencies were discarded as these are associated with the large amplitude motion of internal rotation. The barrier heights of the hindered internal rotation were calculated by altering the torsion angle and calculating the energy, and determining the difference between highest and lowest values. Variation of calculated *tert*-butoxy vibrational frequencies by $\pm 10\%$ produces only a slight variation ($<5\%$) in the best fit parameters which is within other experimental and calculational errors.

The vibrational frequencies, internal and external moments of inertia were used to calculate a density of states for the *tert*-butoxy reagent.[27] Microcanonical rate coefficients [$k(E)$] were obtained by inverse Laplace transformation of an Arrhenius expression for the decomposition reaction and incorporated into a master equation to calculate the canonical rate coefficient of the reaction under experimental conditions. Collision frequencies were calculated using tabulated data[28] for helium and for *tert*-butoxy, by analogy with similar molecules. The calculated fits were insensitive to changes in these estimated parameters. The other parameter required in the master equation is $\langle \Delta E_d \rangle$, the average energy transferred in a downward collision. This parameter was allowed to float in the fit.

The fit was performed by comparing the calculated (k_{calc}) and experimental (k_{expt}) data over the complete T, p range with the use of a χ^2 function

$$\chi^2 = \sum_{T,p} \frac{1}{\sigma^2} (k_{calc} - k_{expt})^2$$

where σ^2 is the variance associated with each experimental measurement. The nature of the χ^2 surface and complexity of the calculation (numerical derivatives required) renders conventional Marquardt techniques inefficient. We have therefore conducted a grid search varying A_2^{∞}, E_2^{∞} and $\langle \Delta E_d \rangle$ over a range of conditions compatible with previous experimental determinations. Fig. 5 shows the χ^2 surface as a function of A^{∞}, E^{∞} for $\langle \Delta E_d \rangle = 150$ cm^{-1}, and the solid lines in Fig. 4 are the fit to the experimental data with the best fit parameters of: $A^{\infty} = 1.4 \times 10^{13}$ s^{-1}, $E^{\infty} = 57$ kJ mol^{-1} and $\langle \Delta E_d \rangle = 150$ cm^{-1}. The wells reflect the relatively coarse grid used; the insert in Fig. 5 shows the surface in more detail

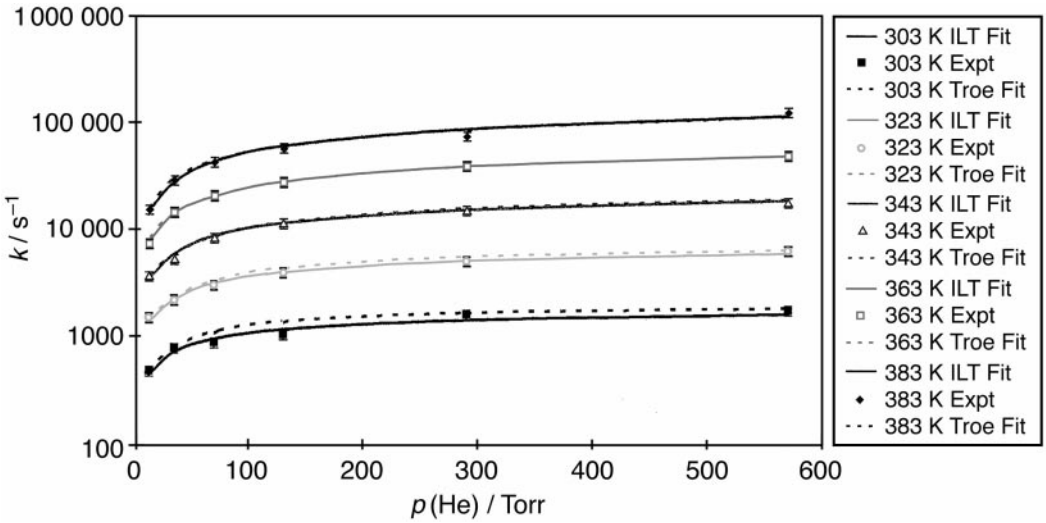

Fig. 4 Pressure dependence of the first order rate coefficient at 303, 323, 343, 363 and 383 K with ILT–ME (solid lines) and Troe (dashed lines) fits to the data.

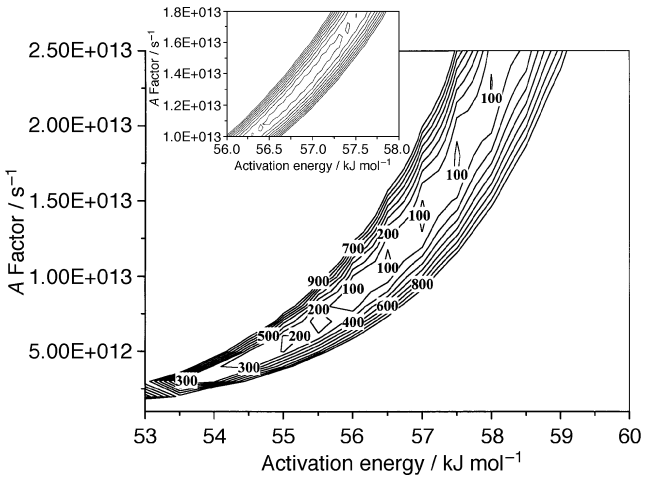

Fig. 5 χ^2 surface for a fixed value of $\Delta E_d = 150$ cm^{-1}. A_2 has been varied from 1×10^{12}–2.5×10^{13} in steps of 1×10^{12} s^{-1}. E_2 has been varied from 53–60 kJ mol^{-1} in steps of 0.5 kJ mol^{-1}.

around the minimum. The quality of the fit is excellent, the χ^2 value corresponding to an average deviation for each datum point of less than 6%, comparable with the experimental error associated with that measurement ($\sim$10%). The χ^2 surface is relatively flat close to the minimum and the nature of the surface shows that the fitting parameters are correlated. Based on the shape of the χ^2 surface and uncertainties in the experiments and calculations, we estimate the following range of best fit parameters from the ILT-ME method as:

$$A_2^\infty = (1.4 \pm 0.6) \times 10^{13}\ \text{s}^{-1};$$

$$E_2^\infty = (57 \pm 2)\ \text{kJ mol}^{-1};$$

$$\langle \Delta E_d \rangle = (150 \pm 20)\ \text{cm}^{-1}$$

Table 2 summarises the current measurements and the literature values. The Arrhenius parameters are lower than previous determinations and recommendations and this is discussed following the Troe analysis. The resulting value of $\langle \Delta E_d \rangle$ is lower than the values of $\sim$200 cm^{-1} observed in the higher temperature alkyl decompositions.[29–31] However, careful studies[32] have indicated that $\langle \Delta E_d \rangle$ shows a positive temperature dependence and the values of $\langle \Delta E_d \rangle$ from the *tert*-butoxy system are probably compatible with the higher temperature work suggesting that $\langle \Delta E_d \rangle$ is independent of the nature of the radical.

An alternative method of fitting is *via* the methodology proposed by Troe.[21–23] The data are treated globally (*i.e.* all fall-off curves fitted simultaneously) with the Troe parameters k^0, k^∞ modelled by an Arrhenius function and F_{cent}, the parameter describing the broadening of the Lindemann Hinshelwood fall off, being fitted as

$$F_{cent} = C(T/300)^n$$

Each fall off curve could have been fitted individually, but this introduces too much flexibility into the fitting. Previous studies, for example Wagner and Wardlaw,[33] have used more complex parameterizations of F_{cent}, however, these have generally been for association reactions covering a much wider range of temperature. For the limited temperature covered in this dissociation study only a simple parameterization of F_{cent} is justified.

The resulting fits are shown as the dotted lines in Fig. 4 and the fitting parameters are summarised in Table 2. Fits of comparable quality can also be achieved by fixing the high pressure limiting values of A_2^∞ and E_2^∞ at the values determined in the ILT-ME method and floating only F_{cent} and k_2^0.

One of the surprising features of this reaction is that it is indeed pressure dependent. Gutman and co-workers[29] have studied the decomposition of the neopentyl radical;

$$(CH_3)_3CCH_2 \rightarrow (CH_3)_2C : CH_2 + CH_3 \qquad (4)$$

which might be expected to show similarities with the *tert*-butoxy system, and found it to be at 65% of the high pressure limit at 18 Torr of helium at 560 K. At 400 K (close to the highest temperature in this study) 98% of high pressure limit is predicted to be reached at a mere 1 Torr. In contrast the *tert*-butoxy system is well into the fall-off regime at lower temperatures and higher pressures.

The differences in fall-off characteristics for the potentially similar neopentyl and *tert*-butoxy systems can be rationalised by examination of the RRKM expression for the microcanonical rate coefficient $k(E)$:[15]

$$k(E) = \frac{W(E^+)}{h\rho(E)}$$

where $W(E^+)$ is the number of rovibrational levels in the transition state and $\rho(E)$ is the density of states of the reagent radical. For a given energy above the threshold, $W(E^+)$ will be similar for both systems, however, because of the much greater threshold energy for neopentyl (129 kJ mol^{-1})[29] the density of states in the neopentyl radical will be orders of magnitude greater than for the *tert*-butoxy and the microcanonical rate coefficient correspondingly lower. With a much lower dissociation rate, a Boltzmann distribution of energised states can more readily be achieved and hence the high pressure limit is reached at significantly lower pressures in the neopentyl system.

Semi-quantitative confirmation of this argument can be achieved with the current ILT–ME model. As a first-order approximation we use the same frequencies for the two systems, but input the Arrhenius parameters to match the *tert*-butoxy ($A = 1.4 \times 10^{13}$ s^{-1}, $E_a = 57$ kJ mol^{-1}) and neopentyl ($A = 8 \times 10^{13}$ s^{-1}, $E_a = 129$ kJ mol^{-1})[29] systems. Microcanonical rate coefficients are calculated using the ILT formulation of $k(E)$:[15]

$$k(E) = \frac{A\rho(E - E^0)}{\rho(E)}$$

where E^0 is the threshold energy and Fig. 6(a) shows the reduction in magnitude of $k(E)$ for the neopentyl system. Inputting the $k(E)$s into the ME with a constant $\langle \Delta E_d \rangle$ of 150

Table 2 Arrhenius parameters for *tert*-butoxy decomposition

Data	$A/10^{13}$ s^{-1}	E_a/kJ mol^{-1}	k_{298}/s^{-1}
k_2^∞ from ILT-Me fitting	1.4 ± 0.6	57 ± 2	1430
k_2^∞ from Troe fitting[b]	0.35 ± 0.04[a]	53.1 ± 0.3[a]	1722
k_2^0 from Troe fitting[b]	2.1[c] ± 0.5[a]	32.5 ± 0.7[a]	
Batt and Robinson 1987[7]	39.8	67.0	717
Batt *et al.* 1989[8]	11	62.5 ± 0.6	1218
Choo and Benson 1981[34]	13	64.0	762
Atkinson 1997[1]	60	67.7	814

[a] The reported errors here are statistical only ($\pm 1\sigma$). [b] $F_{cent} = (0.395 \pm 0.025)(T/300)^{(1.13 \pm 0.22)}$. [c] Units 10^{-9} cm^3 molecule^{-1} s^{-1}.

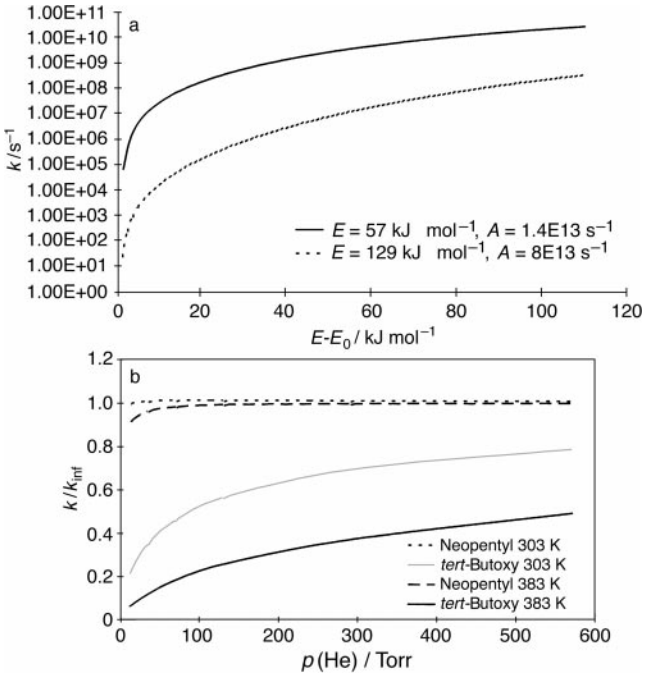

Fig. 6 (a) Microcanonical rate coefficients for the *tert*-butoxy system returned by the ILT model as a function of input Arrhenius parameters, showing considerable reduction in $k(E)$ for values corresponding to neopentyl decomposition. (b) Reduced fall off curves at 303 and 383 K for Arrhenius parameters corresponding to *tert*-butoxy and neopentyl decomposition.

cm^{-1} gives the reduced fall off curves shown in Fig. 6(b) confirming the pressure independence of the neopentyl system under these conditions.

The Arrhenius parameters returned from the ILT–ME and Troe fits are significantly lower than previous measurements,[8] thermochemical calculations[34] or the review values of Atkinson.[1] Support for the significantly lower Arrhenius parameters measured in this work comes from a recent direct study on isopropoxy decomposition using a similar laser flash photolysis-LIF technique.[35]

$$(CH_3)_3HCO \rightarrow CH_3CHO + CH_3 \qquad (5)$$

An Arrhenius analysis of data taken over the pressure range 10–50 000 Torr gives the following parameters:

$$k_5^{\infty} = 9.3 \times 10^{13} \exp(-63.7 \text{ kJ mol}^{-1}/RT) \text{ s}^{-1}$$

A possible partial explanation for the higher parameters reported in the previous relative rate work[8] can be found by examining the temperature dependence of the reference reaction with NO. Batt *et al.* have used a temperature independent rate coefficient for this reaction of 4.2×10^{-11} cm^3 $molecule^{-1}$ s^{-1} calculated using thermochemical methods, whereas the direct measurements reported above show that the reaction has a negative temperature dependence and values lower than that used by Batt *et al.* over their experimental temperature range of 303–393 K.

Park *et al.*[36] measured a single value of k_2 at 413 K and a pressure of 200 Torr of argon. The reported value of 1.2×10^6 s^{-1} is 50% greater than the high pressure limiting value calculated from the current Arrhenius parameters and it is therefore difficult to reconcile the two measurements.

Over a tropospheric temperature range of 220–305 K the earlier Arrhenius equation of Batt[8] predicts lower decomposition rate coefficients than the present work, varying from ~38% of the value predicted from this work at 220 K (0.16 s^{-1} *vs.* 0.4 s^{-1}) to 90% at 305 K (2174 s^{-1} *vs.* 2420 s^{-1}). A graphical depiction of the Arrhenius parameters is given in Fig. 7. As decomposition is the only significant atmospheric

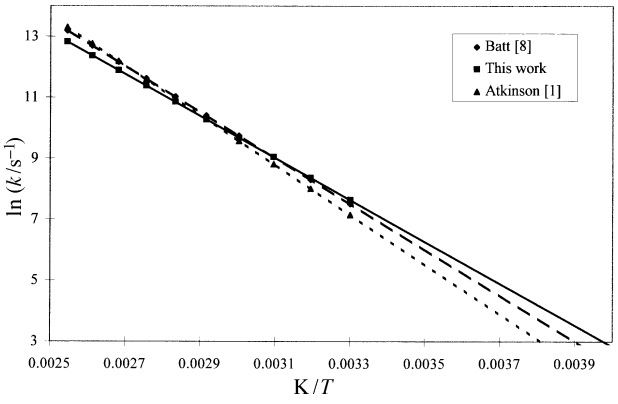

Fig. 7 Arrhenius plot for *tert*-butoxy decomposition. Lines are extrapolations to lower temperatures (solid line, this work; dashed line, Batt *et al.*[8]; dotted line, Atkinson[1])

removal process for the *tert*-butoxy radical, it is unlikely that any re-evaluation of the Arrhenius parameters will have any effect on the predicted atmospheric decomposition mechanism for the *tert*-butoxy radical. The significance of the current Arrhenius parameters is for other alkoxy radicals where there is a significant competition between decomposition and either isomerization or reaction with oxygen. Further experiments on other C_4 alkoxy radicals are currently in progress.

The relatively low value of the pre-exponential factor has mechanistic implications, implying as it does, that the transition state is not as loose as normally expected for a dissociation reaction. The dissociation is more complex than that occurring on a Type II potential such as for ethane decomposition. As well as the cleavage of a C–C bond there is a compensating tightening of the C–O bond and therefore very high A factors would not be predicted, but nevertheless the experimentally determined A factors are considerably lower than thermochemical estimates.[34]

Possible insights into the mechanism come from an examination of the reverse reaction, the addition of methyl radicals to acetone. One might expect the electron deficient methyl radical to preferentially attack the oxygen atom, the *tert*-butoxy radical only being formed following an internal rearrangement. By the principle of microscopic reversibility, this rearrangement must be the first step in the overall decomposition reaction and would be expected to have a significantly lower A factor than a simple decomposition. Thermochemistry would appear to support this mechanism as the enthalpy of formation of the hydroxyalkyl radicals is lower than that of the corresponding alkoxy species. There have been very few studies of addition reactions to carbonyl species, however, one very relevant paper by Sosa and Schlegel[37] investigates the routes of H atom addition to the carbonyl bond in formaldehyde. Here, despite the enhanced stability of the hydroxymethyl radical, addition is predicted to occur *via* attack on the carbon atom of the double bond, evidence against the mechanism postulated above. Alkoxy formation *via* addition reactions would appear to be good subjects for theoretical investigation as the relatively facile abstraction process generally dominates over addition making experimental determinations difficult.

The only reported experimental measurement of methyl addition to acetone is an isotopic study by Knoll *et al.*[38] who looked for the acetone products of methyl scrambling following the addition of methyl radicals to deuterated acetone. However, given that the heat of formation of the *tert*-butoxy radical (-90.7 kJ mol^{-1} giving a reaction endothermicity of 23 kJ mol^{-1}, ref. 20) is correct, the activation energy determined during this study is incompatible with the activation energy of 48 kJ mol^{-1} determined by Knoll *et al.* for the addition of methyl radicals to acetone.

Table 3 Mechanism used to fit NO decay traces

Reaction	k_{282}/cm^3 molecule^{-1} s^{-1}	Reference
t-$C_4H_9O + NO \rightarrow t$-$C_4H_9ONO$ (3)	k_3 floated	
t-$C_4H_9O \rightarrow CH_3 + CH_3COCH_3$ (2)	$k_2 = 565$ s^{-1}	This work
t-$C_4H_9O + t$-$C_4H_9O \rightarrow$ products (6)	k_6 floated	
$CH_3 + CH_3 \rightarrow C_2H_6$ (7)	$k_7 = 6 \times 10^{-11}$	41
$CH_3 + NO \rightarrow CH_3NO$ (8)	$k_8 = 3 \times 10^{-12}$ or 9.7×10^{-12}	42
$NO \rightarrow$	k_{diff}	

VI *tert*-Butyl nitrite photolysis: NO monitoring

In an attempt to further validate the experimental method we have performed a series of experiments at 282 K monitoring the NO time dependence following the photolysis of *tert*-butyl nitrite. The decay traces showed a residual NO concentration in comparison to the pretrigger baseline indicating an alternative removal reaction for *tert*-butoxy other than recombination with NO. A portion of this loss will be due to *tert*-butoxy decomposition which can be accounted for using the Arrhenius parameters generated in section IV. However, the methyl radicals produced in the decomposition reaction may also react with NO and this needs to be considered in the analysis. Decomposition does not fully account for the residual level of NO which in these experiments has been attributed to the *tert*-butoxy + *tert*-butoxy reaction.

Whilst *tert*-butyl nitrite has been used in several studies[8] as a photolytic precursor for *tert*-butoxy radicals, Kades *et al.*[39] have also investigated the vibrational distribution of the NO generated by photolysis around 350 nm. Under these conditions NO is produced vibrationally "hot" with little ($\sim$5%) direct population of ground state $v = 0$. This observation was confirmed during our preliminary experiments. When *tert*-butyl nitrite was photolysed in 100 Torr He little NO ($v = 0$) signal was observed initially, an observation attributed to the inefficiency of helium in vibrationally relaxing NO.[40] Therefore a buffer gas is required that efficiently relaxes the "hot" NO but does not chemically affect the system. CH_4 is known to efficiently relax vibrationally "hot" NO[40] and will not chemically interfere with the chemistry of the system. Therefore *ca.* 2 Torr CH_4 was additionally added to the system. Under these conditions the system is thermalized faster than the chemical change.

Examples of a number of [NO] *vs.* time traces are shown in Fig. 8. These traces show the decay of NO to a non-zero baseline. In order for reaction on the timescale of the experiment a sizeable radical concentration was required. This was achieved by having a high nitrite concentration (*ca.* 25–75 mT), and also by focusing the photolysis light, using a 76 cm focal length lens, such that the photolysis beam measured *ca.* 6 × 3 mm at the reaction zone. This enabled concentrations of between 0.2 and 1.25 mTorr of radicals, RO–NO, to be generated. It was observed that there was a significant residual NO signal present ($\leqslant$0.35 mTorr) in the absence of the photolysis laser. This was attributed to degradation of the nitrite precursor either in the storage bulb or as it passed through the metal manifold–reaction cell. This residual concentration of NO was accounted for within the kinetic analysis. After each experiment the nitrite flow was turned off and a gas mixture of known NO concentration was flown in its place. This enabled the NO signal obtained for each experiment to be converted to an absolute NO concentration. In total, eight experiments were performed at 282 K.

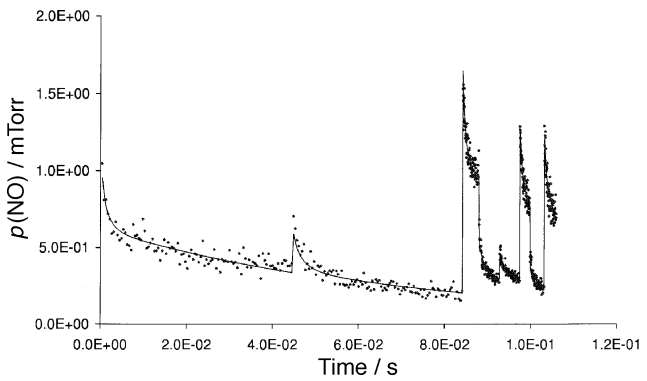

Fig. 8 Typical NO decays following the photolysis of *tert*-butyl nitrite at 282 K. The solid line shows a fit to the data using the parameters generated by a global analysis of all experiments based on Scheme 1.

The data were fitted globally (solid line in Fig. 8) to the kinetic scheme shown in Table 3. From the Arrhenius expression determined in Section V, $k_2 = 565$ s^{-1} CH3 + CH_3 is well determined and can be fixed, 6×10^{-11} molecule^{-1} cm^3 s^{-1}.[40] There is a difficulty with the CH_3 + NO rate constant in that under the experimental conditions the reaction is in the fall-off region. The value for CH_3 + NO in 100 Torr is 3×10^{-12} molecule^{-1} cm^3 s^{-1}, but in our experiments we also added *ca.* 2 Torr of CH_4, and this might significantly push the rate constant towards its high pressure limit of 9.7×10^{-12} molecule^{-1} cm^3 s^{-1}.[42] Diffusion was approximated to a first-order (exponential) loss process; while this is an approximation it does not significantly affect the overall result because diffusional losses are small ($\sim$10 s^{-1}) compared to chemical losses.

The kinetic data were fitted using a program that numerically integrated the above scheme and adjusted the rate parameters, using a Marquardt algorithm, to best fit the data. The program also allowed all eight kinetic traces to be fitted simultaneously, in a global analysis procedure. The datum points were assigned equal weighting. Two kinetic schemes were used. Firstly (Scheme 1), the lower value of reaction (7), corresponding to reaction within the fall-off region was used, secondly (Scheme 2), the addition of 2 Torr of methane was assumed to promote reaction to the high pressure limit. The results of the analysis are presented in Table 4.

The returned values for k_3 are in excellent agreement with the earlier direct determinations ($k_{298} = 2.5 \times 10^{-11}$ cm^3 molecule^{-1} s^{-1}) and do not appear to depend significantly on the values used for the CH_3 + NO reaction. The fitted values for k_6 on the other hand are strongly dependent on the residual level of NO and hence on the competition between reactions (7) and (8). The rate coefficient for reaction (6) is therefore poorly determined in these experiments. Better estimates may be obtained by working at a lower temperature where decomposition is insignificant and any residual NO

Table 4 Returned parameters from numerical fits of NO decay traces

Scheme	$10^{11}k_3$[a]	$10^{11}k_6$[a]	k_{diff}/s^{-1}
1	2.44 ± 0.19	0.60 ± 0.16	16 ± 1
2	2.54 ± 0.20	1.33 ± 0.19	15 ± 1

[a] Units are in cm^3 molecule^{-1} s^{-1}.

should be more directly attributable to the *tert*-butoxy recombination. The time dependence of [NO] following nitrite photolysis at low temperatures is currently under study for all C_4 alkoxy isomers and will be reported in a subsequent paper.

VII Conclusions

A laser-induced fluorescence spectrum has been recorded following the photolysis of *tert*-butylnitrite. Without spectroscopic assignment it is not possible to conclusively attribute the spectrum to the *tert*-butoxy radical, however, the photolysis of alkyl nitrites is reasonably well characterised and the *tert*-butoxy radical is the major expected radical product. Support for the identification of the spectrum comes from the excellent agreement for the rate coefficient for the recombination of the *tert*-butoxy radical with NO as determined by direct monitoring of the LIF signal or from the time dependence of the NO co-photoproduct. Studies on the *tert*-butoxy + NO reaction confirm a negative temperature dependence and yield a room temperature rate coefficient of 2.5×10^{-11} cm^3 molecule^{-1} s^{-1}. These results add to the relatively small body of knowledge on alkoxy + NO reactions and suggest that the recommendations of Atkinson[1] may over-estimate ambient rate coefficients for the reactions of larger alkoxy radicals with NO.

The decomposition of the *tert*-butoxy radical has been studied directly as a function of pressure and temperature. The reaction is in the fall-off regime under the experimental conditions using both a monoatomic bath gas and with an additional polyatomic bath gas (methane). Limiting high pressure rate coefficients were estimated *via* an ILT-ME technique and the Troe factorisation technique. Due to the increased sophistication of the ILT-ME method, we consider the parameters returned from this methodology as our best estimates for calculating k_2^∞. The Arrhenius parameters from this study are significantly lower than those from previous determinations or calculations. High-level theoretical calculations are required for alkoxy radical decompositions as the results of this study seem to indicate that the mechanism could be more complex than expected. Such calculations would be of immense help for both the atmospheric and combustion communities as higher alkoxy and polyfunctional alkoxy radicals (*e.g.* the β-hydroxy alkoxy radicals formed in the atmospheric oxidation of alkenes) are difficult to study experimentally.

Acknowledgements

The authors are grateful for funding from NERC (GST/02/1049) and the European Union (Contract No PL950731).

References

1 R. Atkinson, *Int. J. Chem. Kinet.*, 1997, **29**, 99.
2 R. W. Walker and C. Morley, "Basic Chemistry of Combustion", in *Low Temperature Combustion and Autoignition*, ed. C. Morley and M. J. Pilling, *Comprehensive Chemical Kinetics*, Elsevier, BV, Amsterdam, 1997, vol. 35.
3 Structure Activity Relationships for the Degradation of Biogenic Volatile Organic Compounds (SARBVOC) EU Project PL950731.
4 L. Batt, R. D. McCulloch and R. T. Milne, *Int. J. Chem. Kinet.*, 1975, **7**, 441.
5 L. Batt, *Int. J. Chem. Kinet.*, 1979, **11**, 977.
6 L. Batt and G. N. Robinson, *Int. J. Chem. Kinet.*, 1982, **14**, 1053.
7 L. Batt and G. N. Robinson, *Int. J. Chem. Kinet.*, 1987, **19**, 391.
8 L. Batt, M. W. M. Hisham and M. Mackay, *Int. J. Chem. Kinet.*, 1989, **21**, 535.
9 M. A. Blitz, D. G. Johnson, M. Pesa, M. J. Pilling, S. H. Robertson and P. W. Seakins, *J. Chem. Soc., Faraday Trans.*, 1997, **93**, 1473.
10 R. J. Balla, H. H. Nelson and J. R. McDonald, *Chem. Phys.*, 1985, **99**, 323.
11 M. J. Frost and I. W. M. Smith, *J. Chem. Soc., Faraday Trans.*, 1990, **86**, 1751 and M. J. Frost and I. W. M. Smith, *J. Chem. Soc., Faraday Trans.*, 1990, **86**, 1757.
12 X. Q. Tan, J. M. Williamson, S. C. Foster and T. A. Miller, *J. Phys. Chem.*, 1993, **97**, 9311.
13 P. Devolder SARBVOC 1st Annual Report, European Union, Brussels, 1997.
14 R. Zellner, *J. Chim. Phys.*, 1987, **84**, 403.
15 K. Holbrook, M. J. Pilling and S. H. Robertson, *Unimolecular Reactions*, J. Wiley, Chichester, UK, 1997.
16 L. Batt and R. T. Milne, *Int. J. Chem. Kinet.*, 1974, **6**, 945.
17 G. D. Mendenhall, D. M. Golden and S. W. Benson, *Int. J. Chem. Kinet.*, 1975, **7**, 725.
18 L. Batt and R. T. Milne, *Int. J. Chem. Kinet.*, 1976, **8**, 59.
19 S. W. Benson, *Thermochemical Kinetics*, Wiley–Interscience, New York, 1976.
20 D. F. McMillan and D. M. Golden, *Ann. Rev. Phys. Chem.*, 1982, **33**, 493.
21 J. Troe, *J. Phys. Chem.*, 1979, **83**, 114.
22 J. Troe, *Ber. Bunsen-Ges. Phys. Chem.*, 1983, **87**, 161.
23 R. G. Geiber, K. Luther, and J. Troe, *Ber. Bunsen-Ges. Phys. Chem.*, 1983, **87**, 169.
24 Cerius2, version 3.7, Molecular Simulations Inc., 9685 Scranton Road, San Diego, CA 92121–3752.
25 A. K. Rappe and W. A. Goddard, *J. Phys. Chem.*, 1991, 95, 3358.
26 E. B. Wilson, J. C. Decius and P. C. Cross, *Molecular Vibrations*, Dover, New York, 1980.
27 J. Gang, M. J. Pilling and S. H. Robertson, *J. Chem. Soc., Faraday Trans.*, 1996, **92**, 3509.
28 R. B. Bird, W. E. Stewart and E. N. Lightfoot, *Transport Phenomena*; John Wiley and Sons, New York, 1960, 511.
29 I. R. Slagle, L. Batt, G. W. Gmurczyk, D. Gutman and W. Tsang, *J. Phys. Chem.*, 1991, **95**, 7732.
30 M. A. Hanning-Lee, N. J. B. Green, S. H. Robertson and M. J. Pilling, *J. Phys. Chem.*, 1993, **97**, 860.
31 P. W. Seakins, S. H. Robertson, M. J. Pilling, I. R. Slagle, G. W. Gmurczyk, A. Bencsura, D. Gutman and W. Tsang, *J. Phys. Chem.*, 1993, **97**, 4450.
32 Y. Feng, J. T. Niiranen, A. Bencsura, V. D. Knyazev, D. Gutman and W. Tsang, *J. Phys. Chem.*, 1993, **97**, 871.
33 A. F. Wagner and D. M. Wardlaw, *J. Phys. Chem.*, 1988, **92**, 2462.
34 K. Y. Choo and S. W. Benson, *Int. J. Chem. Kinet.*, 1981, **13**, 833.
35 P. Devolder, Ch. Fittschen, A. Frenzel, H. Hippler, G. Poskrebyshev, O. F. Stiebel and B. Viskolcz, *Phys. Chem. Chem. Phys.*, 1999, submitted.
36 J. M. Park, N. W. Song and K. Y. Choo, *Bull Korea, Chem. Soc.*, 1990, **11**, 343.
37 C. Sosa and H. B. Schlegel, *Int. J. Quant. Chem.*, 1986, **29**, 1001.
38 H. Knoll, G. Richter and R. Schliebs, *Int. J. Chem. Kinet.*, 1980 **12**, 623.
39 E. Kades, M. Rosslein and J. R. Huber, *J. Phys. Chem.*, 1994, **98**, 13556.
40 I. J. Wysong, *J. Chem. Phys.*, 1994, **101**, 2804.
41 I. R. Slagle, D. Gutman, J. W. Davies and M. J. Pilling, *J. Phys. Chem.*, 1988, **92**, 2455.
42 J. W. Davies, N. J. B. Green and M. J. Pilling, *J. Chem. Soc., Faraday Trans.*, 1991, **87**, 2317.

Paper 8/06524A